Performance assessment and improvement of a spilt-and-recombine micromixer for immunomagnetic cell sorting*

Chainarong Chaktranond[**,***], Koji Fukagata[****], Nobuhide Kasagi[**]

** Department of Mechanical Engineering, The University of Tokyo,
Hongo 7-3-1, Bunkyo-ku, Tokyo 113-8656, JAPAN

*** Present Address: Department of Mechanical Engineering, Thammasat University, Rangsit Campus,
Khlong Luang, Pathumthani 12121, THAILAND

**** Department of Mechanical Engineering, Keio University,
Hiyoshi 3-14-1, Kohoku-ku, Yokohama 223-8522, JAPAN

Published in *J. Fluid Sci. Technol.* **3**, 1008-1019 (2008).

Abstract

Performance of a split-and-recombine micromixer (Tan et al., 2005) is assessed by means of numerical simulation. The micromixer is designed for micro cell sorting systems using immunomagnetic beads, of which working principle is lamination of fluid layers. The fluid motion in a complex three-dimensional geometry is simulated by using the finite difference method and the motion of beads is dealt with the one-way coupling Lagrangian particle tracking method. Although the thickness of laminated layers should ideally reduce by the factor of 2^n (where n is the number of unit-mixers connected in series), the present simulation with a realistic geometry shows that the thickness does not reduce that much. Relatively large unmixed regions are formed in the central region, which deteriorate the mixing performance. The size of the unmixed regions and the degree of mixing are quantitatively investigated. Based on the observation, an improved mixer arrangement is proposed. While the original arrangement proposed by Tan et al. (2005) was to simply connect identical unit-mixers, the present arrangement is to alternately connect the original unit-mixer and one with the mirrored geometry. With this modified arrangement, the unmixed region is suppressed and better mixing is achieved.

Key words: Passive mixer, Lamination, Numerical simulation, Lagrangian particle tracking, Design

1. Introduction

Regenerative medicine is attracting attention as an alternative strategy to cure disease and repair organs. In the regenerative medicine, it is often required to extract certain kinds of cells from a sample mixture, e.g., mesenchymal stem cells from blood or bone marrow. One of the efficient techniques for this extraction is to use magnetic beads coated with the antibody corresponding to the antigen emerging on the surface of target cells.(1) This technique is called as the immunomagnetic cell sorting (IMCS). Its principle and procedure of separation is illustrated in Fig. 1. In the first process, magnetic beads coated with an antibody (i.e., immunomagnetic beads) are mixed with the sample, so that they are attached to the target cells. After the mixing, only the cells tagged by the immunomagnetic beads are isolated from the mixture by using magnetic forces. One of the problems in the conventional IMCS equipment is the need of large amount of sample, say on the order of 1

*Received 27 June, 2008 (No. 08-0411)
[DOI: 10.1299/jfst.3.1008]

liter, and the high operation cost. A very small IMCS device, which has a potential to reduce the sample volume, cost, and possible infection, is therefore needed.

A key issue for successful development of such a micro IMCS device is how to achieve effective mixing of immunomagnetic beads and cells in a flow of buffer fluid under a low-Reynolds-number environment. Up to now, different types of mixers have been proposed for micro-scale flows. Those mixers can be classified into two categories: active and passive micromixers. In the active micromixers, mixing is enhanced by various kind of external force, such as magnetic force, [2] dielectrophoresis,[3] and pressure disturbance.[4]Although the external forces can be suitably adjusted when the operating conditions are changed, devices required to produce the external forces make the fabrication process highly complicated. On the other hand, the passive micromixers use the geometrical structure of the conduit, so that the stretching and folding of fluids are induced by the chaotic advection[5,6] or the lamination of interfaces.[7-10] The mixers using the latter mechanism, which are called lamination mixers or split-and-recombine (SAR) mixers, can simplify the fabricating and operating processes as compared to the active mixers.

In order to optimize the design of micro mixing devices, the flow characteristics and the resulting mixing performance should be investigated in detail. Numerical simulation has a merit for that purpose, because all the detailed information, such as the location of individual particles, is available even though the mixer has such a complex geometry that cannot easily be accessed by experimental measurement. An example of such numerical simulations is that reported by Hamanaka and Kato.[10] They reported that a cross-SAR configuration accelerates the mixing by 4.4 times as compared to the flow in a straight channel with the same pressure drop. The objective of the present study is to numerically investigate the relationship between the particle motion and the performance of another type of SAR micromixer[9] and to propose an improved design based on the knowledge obtained from the simulation.

2. Split-and-recombine micromixer

We consider an SAR micromixer proposed by Tan et al.,[9] as shown in Fig. 2(a), which has a three-layer structure. The merit of this mixer is its easier fabrication than the other already-proposed mixers which have a complicated three-dimensional geometry: each layer is fabricated separately by using the soft lithography process, and these three layers are simply bonded together. One unit of the micromixer (hereafter called as a unit mixer) is 800 μm long (L_x), and has a constant cross-sectional area of 200 × 200 μm^2 ($L_y \times L_z$) everywhere. As schematically shown in Fig. 2(b), the principle of mixing is to split the flow of two fluid layers perpendicularly to the interface and then stack them. Ideally, if the flow

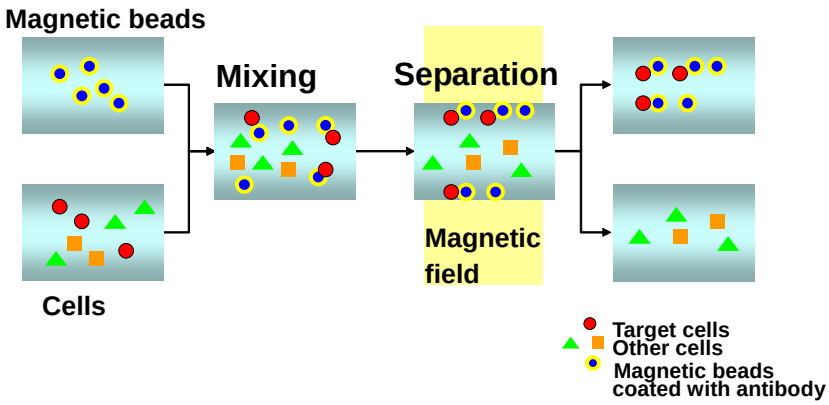

Fig. 1 Schematic of immunomagnetic cell sorting system (IMCS).

Vol. 00, No. 0, 2005

(a)

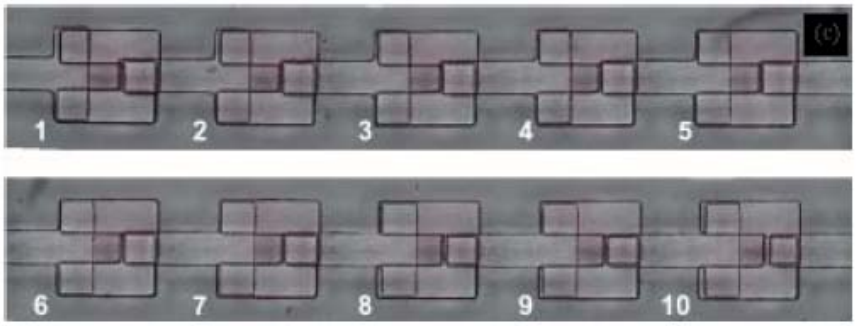

(b)

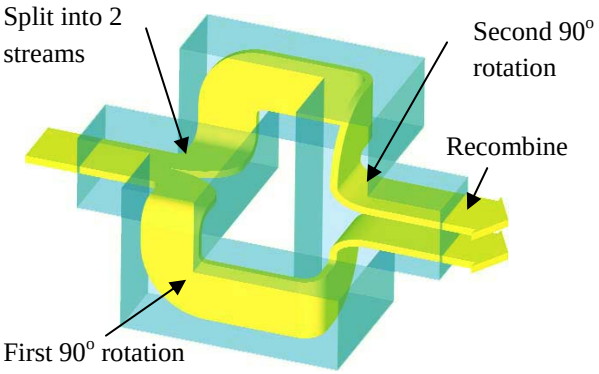

Fig. 2 The SAR micromixer proposed by Tan et al.[9]: (a) fabricated mixer consisting of 10 unit mixers, (b) schematic of a unit mixer.

is completely uniform, the thickness of each fluid layer becomes half after passing a unit of mixer. Namely, when an entire mixer is composed of n unit mixers connected in series, the number of fluid layers increases by 2^n. In addition, this specific micromixer[9] is designed to reduce the sedimentation of magnetic beads, of which density is usually higher than that of the buffer fluid. This is done by designing the branch channels so that the streamlines are rotated by 180 degrees.

3. Numerical procedure

Numerical simulation is used for analyzing the mixing of magnetic beads and cells in a steady laminar flow of micromixer. We consider an incompressible flow of Newtonian fluid at the Reynolds number (*Re*) of 1, 24, and 66. Here, the Reynolds number is defined by using the half height of the inlet section and the bulk-mean velocity at the inlet. The continuity and Navier-Stokes equations are numerically solved by using the second-order-accurate central finite-difference method on a staggered grid system. The immersed boundary method[11] is employed to deal with the complex geometry. The entire computational domain (i.e., including the obstacle region) of a unit mixer is 8δ, 6δ, and 6δ in the streamwise (x), lateral (y), and perpendicular (z) directions, respectively, where δ is a half width of the main channel. The numbers of computational grids are 96×72×72, in x, y, and z directions, respectively. The steady flow field is obtained as a steady solution of the time-dependent simulation. In order to check the accuracy of simulation, we have made computations with four different resolutions, i.e., 48×36×36, 64×48×48, 96×72×72, and 128×96×96. As compared to the values computed in the finest case (i.e., 128×96×96), the bulk-mean velocity computed under a given pressure gradient is found to be within 5% error in all cases, and the maximum velocity in each direction is within 5% error in the case

of 96×72×72 (the resolution used hereafter).

In order to study the motion of immunomagnetic beads and cells as well as their mixing, one-way coupling Lagrangian particle tracking simulation is performed on the computed steady fluid velocity field. Collisions between particles are neglected. We assume, for simplicity, that both beads and cells (referred hereafter as particles, unless specified) are rigid spheres of $d_p = 1$ μm in diameter, although in reality the target cells are deformable and their typical diameters is on the order of $d_p = 10$ μm. The density of beads and cells are $\rho_p = 1500$ and 1000 kg/m^3, respectively. The relaxation time of beads and cells, $\tau_p = d_p^2 \rho_p / (18 \rho_f \nu)$ is on order of $\tau_p \sim 1 \times 10^{-7}$ s and it is much shorter than the time scale of flows considered here. In addition, the gravitational force is neglected for simplicity. Thus, the particle equation of motion[12] is reduced to read

$$\frac{d\vec{u}_p}{dt} = \frac{1}{\tau_p}\left(\vec{u}_f - \vec{u}_p\right), \tag{1}$$

where $\vec{u}_f$ and $\vec{u}_p$ are fluid and particle velocities, respectively. The fluid velocity at the particle position is interpolated from the computational grid points by using the trilinear interpolation scheme. The time integration of the velocity and position of particles is done by using the Crank-Nicolson scheme.

At the inlet, 3200 cells and 3200 magnetic beads are uniformly introduced in the upper and lower halves of the cross-section, respectively. The velocity field computed in the unit mixer is copied to the different mixer units and used for the computation of particle trajectories. Simulation is continued until most of the particles exit from the 11th mixer unit (denoted as Unit 11). Due to the limitation of computation time, the number of particles exited from the outlet varies from case to case. For *Re* = 1 in the original mixer presented in Section 4, it is 82% of the number of particles introduced from the inlet; for the rest of the cases, i.e., *Re* = 24 and 66 in the original mixer (Section 4) and *Re* = 1 in the modified mixer (Section 5), it is 88%, 93% and 89%, respectively.

4. Results and discussion

First, we examine the Poincaré section in order to illustrate the chaotic particle motion in the transverse directions. The horizontal and vertical axes are made dimensionless by using the duct half-width. Note that each red or blue point represents the particle position only, but not the diameter of each particle. Although the centers of different points do not overlap each other, they seem to be overlapping in the figure just because they are plotted with a visible diameter. Especially, when a red particle is close to a blue particle, the red point hides a part of blue point plotted earlier. We also note that the white parts observed in the figure correspond to the regions where no particles have passed in the finite computational time. The Poincaré section in the present study is constructed by tracking the trajectory of particles and plotting their locations in a cross-section at the exit of each mixer unit. By labeling the particles with different colors, i.e., blue for the magnetic beads and red for the cells, we can clearly see the development of mixing and also determine the number of mixer units required for achieving a sufficient mixing.

Figure 3 show the Poincaré sections in the case of *Re* = 1. As has been shown in Fig. 2(b), the number of stacked layers should ideally be doubled when the fluids pass through a mixer unit. However, as can be found from Fig. 3, the lamination layers are significantly distorted. This is due to the non-uniformity and complexity of the velocity field due to the existence of many sharp bends in the mixer. Moreover, in the downstream units, we find several unmixed regions where particles of the same species (i.e., red or blue particles) are locally accumulated. This structure is stable and it deteriorates the overall mixing performance.

In order to illustrate the behavior of these unmixed regions more clearly, only the

Vol. 00, No. 0, 2005

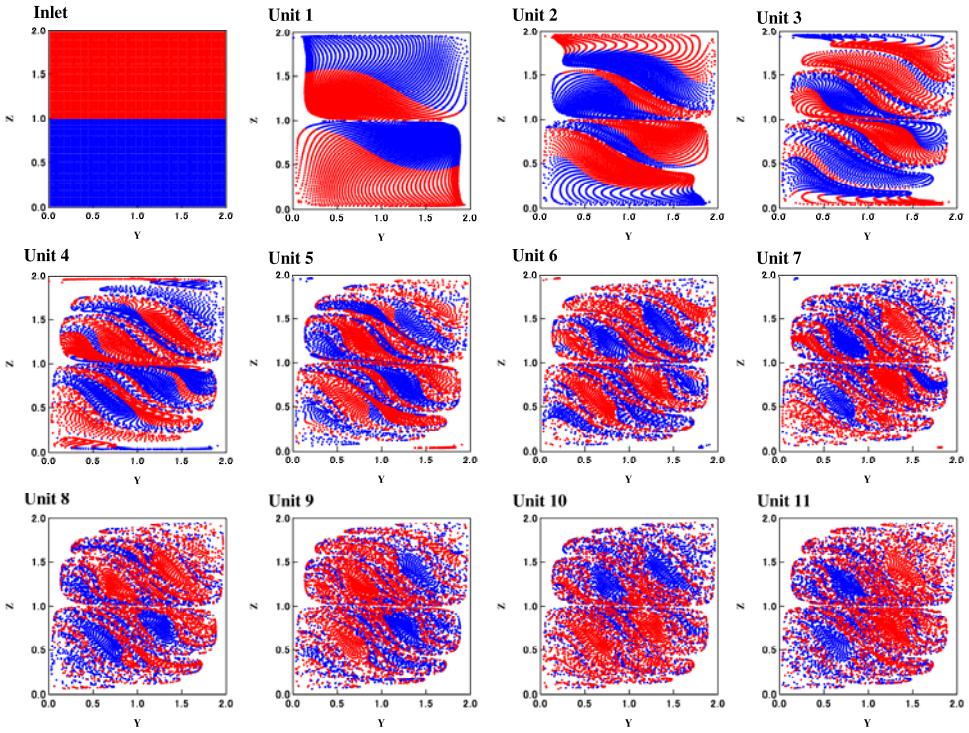

Fig. 3 Distribution of particles at the exit of every mixer unit (i.e., Poincaré section) at *Re* = 1, viewed from the downstream side.

movement of the particles introduced in the lower-left region is depicted in Fig. 4(a). It is found that the ensemble of particles rotates in the anticlockwise direction with a period of four mixer units. Moreover, the particle cloud is found to be self-rotating with a period of two mixer units. Detailed investigation reveals that this self-rotation is also in the anticlockwise direction. One can notice that from Unit 1 to Unit 2 one line of particles departs from the rest of the particles. This phenomenon can be explained by a comparison with the expected change of topology in the case of ideal lamination, in which the fluid layers are simply split and stacked, as shown in Fig. 4(b). In the ideal case, the particles shown in Fig. 4(a) initially belong to the regions labeled as 38, 39, 42, and 43 (enclosed by a red dashed line) in Fig. 4(b). In the case of ideal lamination, this region should be split into the upper right and lower left regions at the exit of Unit 2, as illustrated in Fig. 4(b). Namely, the particles should be split exactly into half. However, in the actual case, the motion of particles is biased to one side. This bias can be attributed to the distortion in the velocity field. One can also suspect that this bias may also be due to different flow rates in the branch channels. According to the computational results, however, the flow rates in the two branch channels are nearly equal (i.e., difference between the flow rates being less than 0.5% of a half of the total flow rate at all Reynolds numbers presented here); thus, the imbalance of flow rates cannot be considered as the reason for this bias.

Figure 5 shows the discrete trajectory of a sample particle starting from (y, z) = (0.6, 0.6), which is considered to be in the center of the above-mentioned self-rotation. As can be found in the figure, the particle comes back to the same locations exactly every four mixer units. This confirms that the motion observed in Figs. 3 and 4 has a periodicity of four mixer units.

Based on the observation above, the motion of the unmixed regions can be schematically illustrated as shown in Fig. 6. A particle cloud in a confined region is convected with an anticlockwise rotation (viewed from the downstream side) and the particles around the periodic point are also rotating around it. Such a tube-like unmixed

(a)

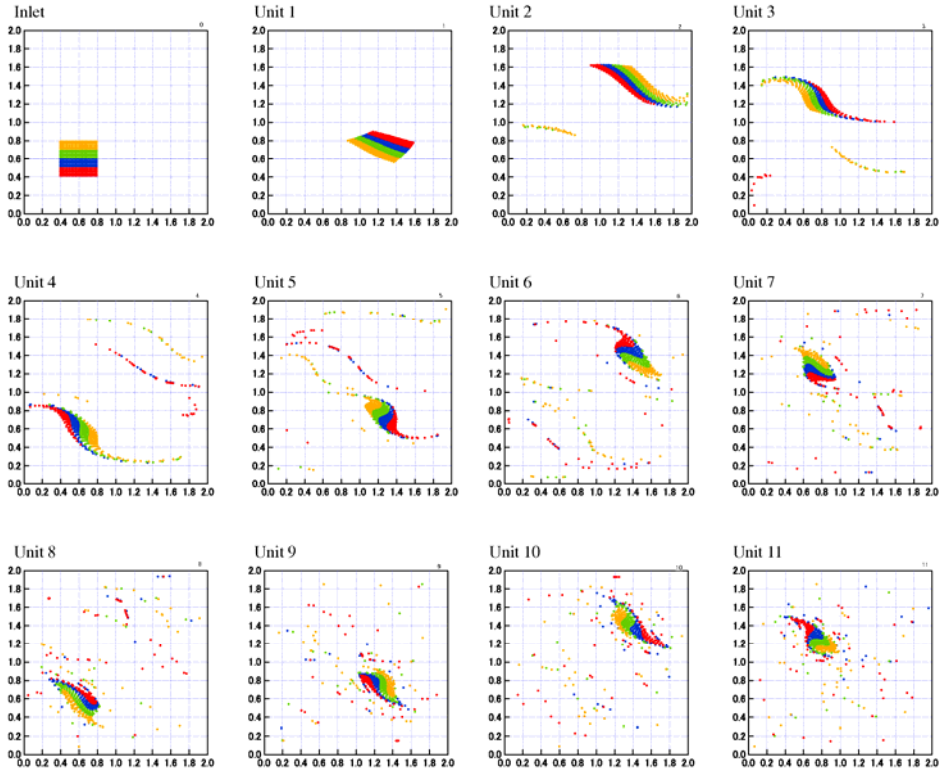

(b)

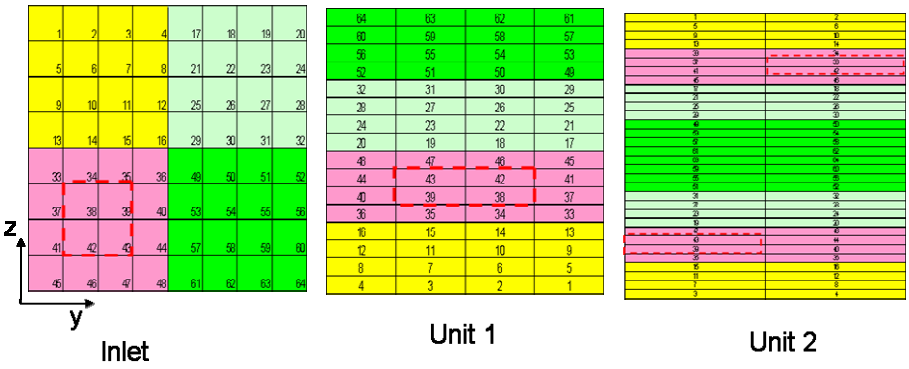

Fig. 4 (a) Movement of the particles initially located in the lower-left region (*Re* = 1), viewed from the downstream side; (b) expected topology in the ideal lamination.

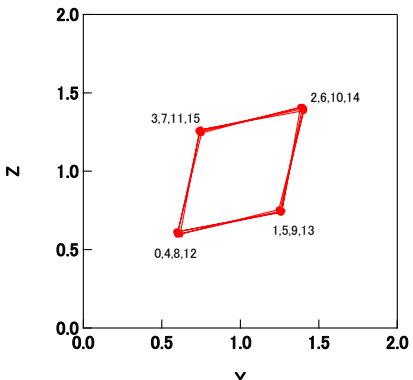

Fig. 5 Movement of periodic point initially located at (*y*, *z*) = (0.6, 0.6). The labels 0-15 denotes the unit number.

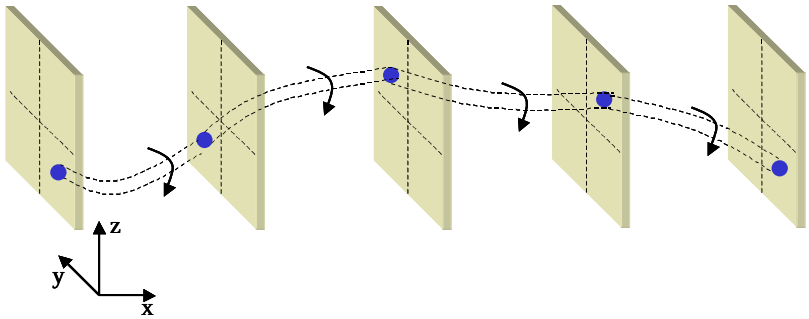

Fig. 6 Schematic of the movement of a periodic island in the present lamination mixer.

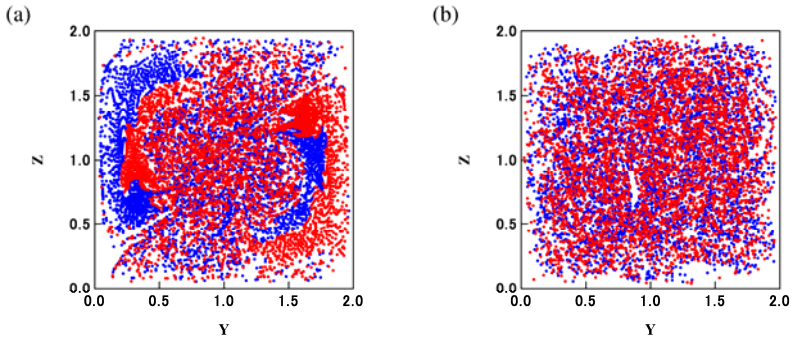

Fig. 7 Distribution of particles in the exit plane of unit 9: (a) *Re* = 24; (b) at *Re* = 66.

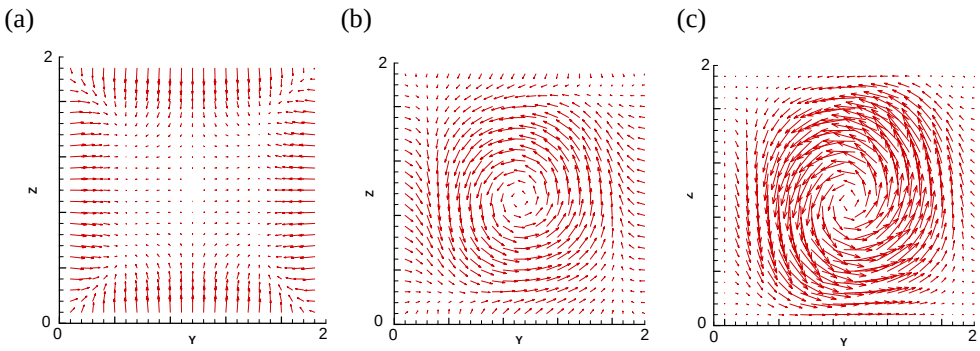

Fig. 8 Velocity vectors in the cross-section at the end of mixer unit: (a) *Re* = 1 (vectors are magnified so as to be visible); (b) *Re* = 24; (c) *Re* = 66.

region is often found in other chaotic systems and is so-called Kolmogorov-Arnold-Moser (KAM) curve/surface.[13]

Figure 7 shows the Poincaré section at *Re* = 24 and *Re* = 66 and Fig. 8 shows the secondary flow in the cross-section. The secondary flow is unidirectional (anti-clockwise) in the cross-section and its magnitude (i.e., the maximum in-plane velocity) is 3%, 8%, and 40% of the bulk-mean velocity in the case of *Re* = 1, 24, and 66, respectively. The secondary flow is considered to work as continuously shifting the phases of red and blue islands so as to prevent the formation of periodic motion. The Poincaré section (Fig. 7) is found to be somewhat different at higher Reynolds numbers. At *Re* = 24, the unmixed regions move close to the wall due to a secondary flow as shown in Fig. 8(b) and the mixing around the center of conduit is better than the case of *Re* = 1. However, the effect of secondary flow is not strong enough so that unmixed regions still remain. At *Re* = 66, no unmixed region is found, which indicates a good mixing. Namely, at higher Reynolds numbers, mixing is enhanced by a secondary flow as shown in Fig. 8(c) in addition to the splitting-and recombination mechanism.

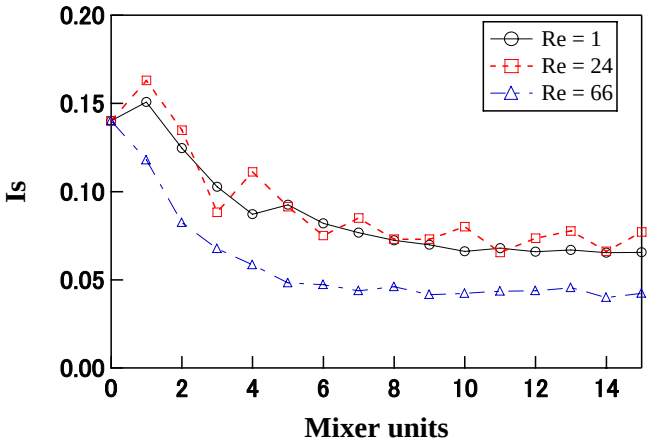

Fig. 9 Entropy index, I_s, computed at the exit of each mixer unit.

The mixing performance is quantified by using two different measures: one is the commonly-used Shanon entropy index[14,15] and the other is the thickness of unmixed region. Note that, despite the difference in the density assumed for the cells and magnetic beads, both particles are found to almost exactly follow the fluid motion due the very short relaxation times. Therefore, the mixing indices are computed only for the mixing of magnetic beads (i.e., blue particles in Fig 3). The mixing indices for the cells (i.e., red particles) take the same values as those for the magnetic beads.

The Shanon entropy index, I_s, used here is that proposed by Phelps and Tucker,[14] which is defined as

$$I_S = 1 - \frac{S}{S_e}, \tag{2}$$

where

$$S = -\sum_{i=1}^{M} \frac{c_i}{N} \ln \frac{c_i}{N} \tag{3}$$

is the Shanon entropy[15]. Here, N is total number of particles in a cross section, M is the number of subdividing bins, and c_i is number of beads included in i-th subdividing bin. The normalization factor in Eq. (2), i.e.,

$$S_e = \ln M \tag{4}$$

is the entropy in the case of uniform mixing.

Figure 9 shows the entropy index, I_s. Here, 10×10 subdividing bins (i.e., M = 100) are used. The index decreases in the first ten mixer units, but it is nearly constant in the downstream units. Similar curves are obtained at Re = 1 and Re = 24, which confirms that the mixing enhancement by the secondary flow is negligibly small at this Reynolds number range. At Re = 66, the entropy index I_s takes smaller values (i.e., better mixing) due to the formation of a strong secondary flow.

Although the entropy index above is a common index used for mixing, it has some problems: (1) it does not give a clear idea on the size of the unmixed islands observed above; (2) it largely depends on the number of subdividing bins used; (3) use of many subdividing bins gives fluctuations in the quantity as has been observed in Fig. 9, while use of small number of bins does not capture the change of mixing property. Therefore, another measure is proposed here. This measure is hereafter called as the average thickness of unmixed regions. The procedure to calculate this thickness is as follows. First, the distance from i-th magnetic bead to the nearest cell in the cross-sectional area, r_i, is computed by

$$r_i = \min_j \left\| \vec{x}_{\text{bead},\, i} - \vec{x}_{\text{cell},\, j} \right\|, \tag{5}$$

where $\vec{x}_{\text{bead},\, i}$ and $\vec{x}_{\text{cell},\, j}$ are the positions of i-th bead and j-th cell, respectively, and $\|\bullet\|$

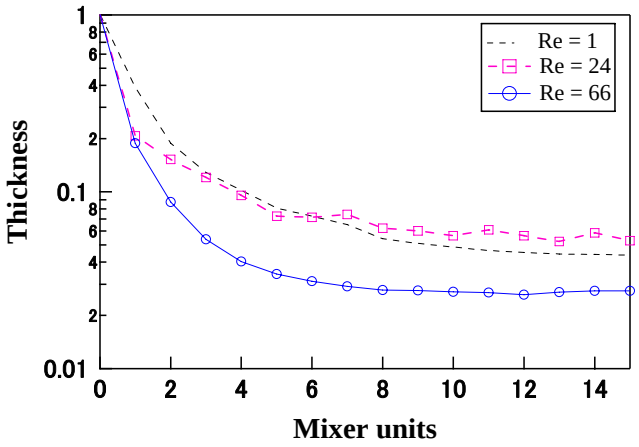

Fig. 10 Variation of average thickness of unmixed regions, 2<*r*>.

denotes the geometric distance. The mean radius of unmixed island is then computed by averaging r_i, i.e.,

$$\langle r \rangle = \frac{1}{N_\mathrm{p}} \sum_{i=1}^{N_\mathrm{p}} r_i \,, \tag{6}$$

where N_p is the number of magnetic beads in each Poincaré section. The average thickness (or diameter) of fluid layers is defined here as $2\langle r \rangle$. Note that, in the limit of $N_\mathrm{p} \to \infty$, the distance between a bead of which height from the bottom wall is z and the nearest cell is given by $r(z) = 1 - z$, with z being made dimensionless by using the duct half-width. Thus, the dimensionless thickness at the inlet can be computed as

$$2\langle r \rangle_{\mathrm{inlet}} = 2\int_0^1 r(z)dz = 2\int_0^1 (1-z)dz = 1. \tag{7}$$

An advantage of this measure over the conventional ones, e.g., the entropy index introduced above, is that by definition this does not largely depend on the sample size: it has an error on the order of distance between nearest particles only.

Figure 10 shows the average thickness, 2<*r*>. The trends are basically similar to those observed in the entropy index. It is clear again that increasing the number of mixer units more than about 10 units does not improve mixing. At *Re* = 1 and *Re* = 24, the average thickness has an asymptotic value of 0.05 – 0.06. This value indicates that the initial blobs have, on average, reduced their thickness by 20 times. At *Re* = 66, the thickness is about half as compared to the cases of *Re* = 1 and *Re* = 24.

The analyses above are made based on the Poincaré sections that do not account for the information of time. For a flow-through-type mixer (like the present mixer) in practice, however, the motion of particles in the high-speed region is more importance. One may thus make a measure of mixing by weighting the quantities by the streamwise velocity, which is analogous to the calculation of mixing cup temperature. We note here, however, that the same conclusion as above can be drawn in the case where the fluid-layer thickness is defined with such velocity weighting.[16]

5 Improvement of mixer arrangement

Based on the observation and analysis above, we propose a new arrangement of SAR micromixers in order to enhance mixing at lower Reynolds numbers. As shown in Fig. 11, the unit mixers with mirrored geometry are connected every two units so that the direction of rotation alternately changes. The present modification is similar to that adopted in

Kenics® partitioned-pipe mixer,[13,17] which has counter-rotating twists in the pipe and drastically reduced the volume enclosed by the KAM surfaces as compared to that in the co-rotating partitioned-pipe mixer.

Figure 12 show the Poincaré sections with the modified mixer at *Re* = 1. As can be noticed, the lamination pattern is closer to the ideal situation and the unmixed region observed in the original mixer seems to have been vanished. Figure 13 depicts the movement of a particle which passes through one of the periodic points observed in the original mixer. Again, in the modified mixer, the particle seems to have no clear periodic motion and it exhibits random movement in the cross section. As shown in Fig. 14, the asymptotic value of the average thickness, $2\langle r \rangle$, is reduced to 0.025, which is nearly half of that in the original mixer. Moreover, this value is comparable to that at *Re* = 66 in the original mixer.

Similarly to the original mixer, secondary flow is found to be very weak in the modified mixer at *Re* = 1. The pressure drop is unchanged from the original mixer, consistent with the weak secondary flow. That means, twice better mixing is achieved in the modified mixer with the same amount of pressure drop as compared to the original mixer. In the case of

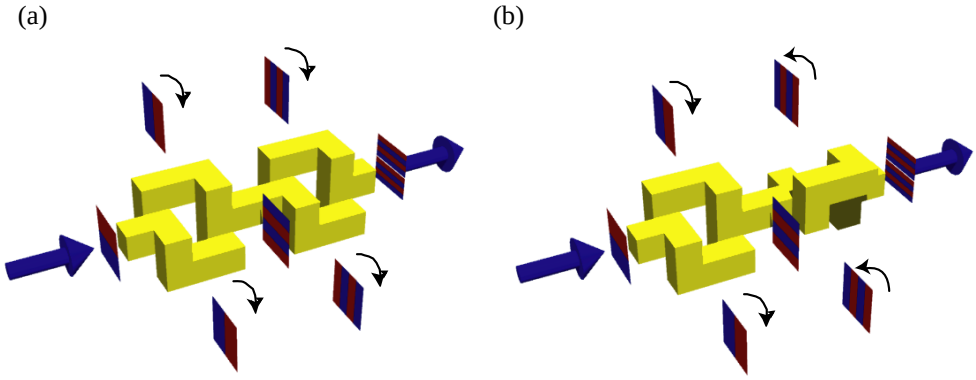

Fig. 11 Mixer arrangements: (a) original[9]; (b) modified (alternating rotation).

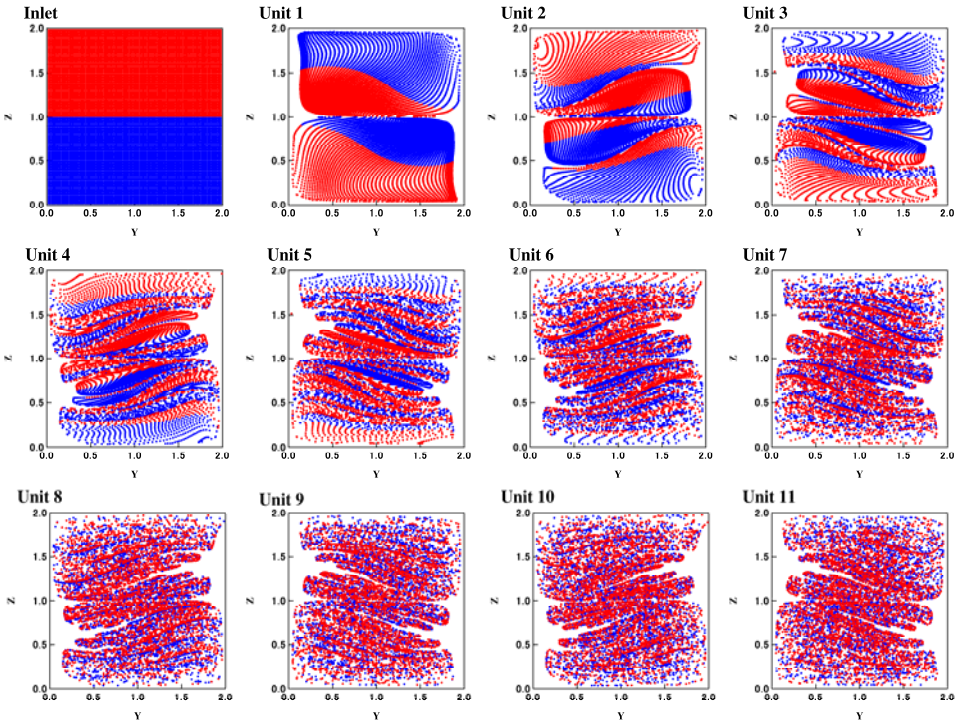

Fig. 12 Poincaré section of the modified mixer (*Re* = 1).

Vol. 00, No. 0, 2005

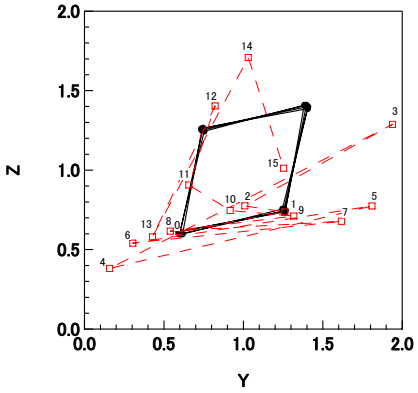

Fig. 13 Comparison of mapping position in the original mixer (solid black line) and that in the modified mixer (dashed red line) (*Re* = 1).

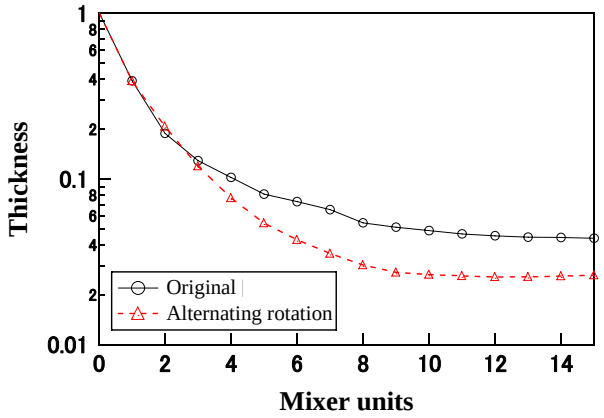

Fig. 14 Average thickness of unmixed islands, 2<*r*>, in the modified mixer (*Re* = 1).

Re = 66 of the original mixer, the periodic islands were destroyed due to the continuous phase change of red and blue islands caused by the secondary flow. In contrast, the improvement in the modified mixer can be attributed to the 180 degree phase-shift that the red and blue islands experience in every mixer unit.

6. Conclusions

Performance of a lamination micromixer proposed for micro magnetic cell sorting systems[9] was evaluated by means of numerical simulation. Although the thickness of lamination layers should ideally decrease by the factor of 2^n, it is found to saturate at a certain level to cause a poor mixing, especially at low Reynolds numbers. Large unmixed regions are found at the Reynolds number of *Re* = 1. These unmixed islands exhibit periodic motion and they form confined stream surfaces known as the KAM surfaces. This causes the prevention of mixing. With increasing the Reynolds number, these unmixed islands tend to be destroyed due to the secondary flows and thereby mixing is improved.

Based on the observation above, we proposed a modified mixer arrangement, i.e., an alternating rotation mixer, so that the fluids are not folded at the same position. Numerical simulation confirms that the unmixed islands are destroyed and thereby the mixing is improved. According to the quantitative measure introduced here, i.e., average thickness, the improved mixer operated at a low Reynolds number (*Re* = 1) is found to have as good mixing performance as the original mixer operated at a higher Reynolds number (*Re* = 66). Finally, it is worth noting that the merit of Tan et al.'s mixer[9], i.e., the easiness of fabrication, is kept unchanged by the present modification of mixer arrangement.

Acknowledgments

The authors are grateful to Drs. Yuji Suzuki and Jun-ichi Miwa (Department of Mechanical Engineering, The University of Tokyo) for helpful comments and fruitful discussions. The authors also thank two anonymous reviewers for their valuable comments that led to significant improvement of paper. This work was supported through the Grant-in-Aid for Scientific Research (S) and the University of Tokyo 21st Century COE program "Mechanical Systems Innovation," by the Ministry of Education, Culture, Sports and Technology of Japan (MEXT).

References

(1) Chalmers, J. J., Zborowski, M., Sun, L., and Moore, L., Flow through immunomagnetic cell ceparation, *Biotechnol. Prog.* Vol. 14 (1998), pp. 141-148.
(2) Suzuki, H., Ho, C.M., and Kasagi, N., A chaotic mixer for magnetic bead-based micro cell sorter, *J. Microelectromech. Sys.*, Vol. 13 (2004), pp. 779-790.
(3) Deval, J., Tabeling, P., and Ho, C.H., A dielectrophoretic chaotic mixer, *Proc. IEEE Int. Conf. MEMS '02* (2002), pp. 36-39.
(4) Volpert, M., Meinhart, C.D., Mezic, I., and Dahelh, M., An actively controlled micromixer, *In Proc. ASME Mechanical Engineering International Congress and Exposition, MEMS, Nashiville, TN*, (1999), pp. 483-487.
(5) Lui, R.H., Stremler, M.A., Sharp, K.V., Olsen, M.G., Santiago, J.G., Adrian, R.J., Aref, H., and Beebe, D.J., Passive mixing in a three-dimensional serpentine microchannel, *J. Microelectromech. Sys.*, Vol. 9 (2000), pp. 190-199.
(6) Stroock, A.D., Dertinger, S.K.W., Ajdari, A., Mezic, I., Stone, H.A., and Whitesides, G.M., Chaotic mixer for microchannels, *Science*, Vol. 295 (2002), pp. 647-651.
(7) Branebjerg, J., Gravesen, P., Krog, J.P., and Nielsen, C.R., Fast mixing by lamination, *Proc. IEEE Int. Conf. MEMS '06* (1996), pp. 441-446.
(8) Schönfeld, F., Hessel, V., and Hofmann, C., An optimised split-and-recombine micro-mixer with uniform 'chaotic' mixing, *Lab on a Chip*, Vol. 4 (2004), pp. 65-69.
(9) Tan, W-H., Suzuki, Y., Kasagi, N., Shikazono, N., Furukawa, K., and Ushida, T., A lamination micro mixer for μ-immunomagnetic cell sorter, *JSME Int. J., Ser. C*, Vol. 48 (2005), pp. 425-435.
(10) Hamanaka, O. and Kato, H., Acceleration of mixing and chemical reaction in a passive micro mixer, Proc. JSME Fluids Engineering Conference 2006, Kawagoe, Oct. 28-29, 2006 (2006), Paper 306.
(11) Kim, J., Kim, D., Choi, H., An immersed-boundary finite volume method for simulations of flow in complex geometries, *J. Comput. Phys.*, Vol. 171 (2001), pp. 132-150.
(12) Maxey, M.R., and Riley, J.J., Equation of motion for a small rigid sphere in a non-uniform flow, *Phys. Fluids*, Vol. 26 (1983), pp. 883-889.
(13) Ottino, M.J., *The Kinematics of Mixing: Stretching, Chaos, and Transport*, Cambridge, New York, Cambridge Press (1989).
(14) Shanon, C.E., A mathematical theory of communication, *Bell System Technical Journal*, Vol. 27 (1948), pp. 379-423.
(15) Phelps, J.H. and Tucker III, C. L., Lagrangian particle calculations of diffusive mixing: Limitation and applications, *Chem. Eng. Sci.*, Vol. 61 (2006), pp. 6826-6836.
(16) Chaktranond, C., Performance assessment of micromixers for bio-fluidic processing with magnetic beads, Doctoral Thesis, The University of Tokyo (2006).
(17) Khakhar, D.V., Franjione, J.G., and Ottino, J.M., A case study of chaotic mixing in deterministic flows: the partitioned-pipe mixer, *Chem. Eng. Sci.*, Vol. 42 (1987), pp. 2909 -2926.